J Polym Res (2014) 21:476
DOI 10.1007/s10965-014-0476-6

ORIGINAL PAPER

Using FTIR spectroscopy to study the phase transitions of poly(*N*-isopropylacrylamide) in tetrahydrofuran-d_8/D_2O

Cheng-Wei Tu · Shiao-Wei Kuo

Received: 17 February 2014 / Accepted: 2 May 2014

Abstract In this study we used Fourier transform infrared (FTIR) spectroscopy to investigate the phase behavior of poly(*N*-isopropylacrylamide) (PNIPAM) in mixed solvents comprising D_2O and tetrahydrofuran-d_8(THF-*d*8). The signals of the CH_3 groups of the *N*-isopropyl amide unit and the CH_2 groups on the main chain and those in the amide I region of the PNIPAM provided details about the various hydrophobic and hydrophilic interactions in the mixed aqueous solution. Upon increasing the volume fraction of THF-d_8 (x_v) from 0 to 11 %, coil-to-globule transition occurred as a result of dehydration and hydrophobic interactions among the hydrophobic groups of the PNIPAM chain, followed by induced aggregation and collapse of the PNIPAM chain. When the value of x_v was in the range of 11 to 55 % the hydrophobic groups formed hydrophobic cages that prevented diffusion of D_2O molecules and the formation of hydrogen bonds with the amide I units of the PNIPAM chains. Meanwhile, the hydration sphere of THF-d_8 also hindered the hydrophobic–hydrophobic interactions between THD-d_8 and the PNIPAM; consequently, the PNIPAM chains shrank as they aggregated. The PNIPAM solution was homogenized again at values of x_v greater than 55 %, due to hydrophobic–hydrophobic interactions among the free THD-d_8 molecules and the hydrophobic groups of the PNIPAM. We believe that dehydration of the hydrophobic groups rather than inter- and intrachain hydrogen bonding was the major driving force behind the aggregation and coil-to-globule transitions.

C.-W. Tu
Green Energy & Environment Research Laboratories, Industrial Technology Research Institute, Hsinchu 310, Taiwan

S.-W. Kuo (✉)
Department of Materials and Optoelectronic Science, Center for Functional Polymers and Supramolecular Materials, National Sun Yat-Sen University, Kaohsiung 804, Taiwan
e-mail: kuosw@mail.nsysu.edu.tw

Published online: 21 May 2014

Keywords PNIPAM · Hydrogen bonding · FTIR · Phase transition

Introduction

"Smart" polymers have properties that respond to changes in their environment such that they can swell or shrink upon small variations in temperature, pH or ionic strength [1, 2]. They have potential applications in, for example, drug delivery, separation and bioswitching [3]. Poly(*N*-isopropylacrylamide) (PNIPAM) is one such polymer that can undergo a coil-to-globule transition in response to changes in temperature and solvent composition [4–11]. PNIPAM has found practical applications [12–14] in controlled drug release, immobilization of enzymes and protein purification [15–21] and has been studied for its various effects triggered through changes in solution temperature or the addition of water-miscible solvents. PNIPAM is insoluble in water above its lower critical solution temperature (LCST) of 30–33 °C [22], where its chains collapse and aggregate into bigger globules; below its LCST, PNIPAM is soluble in an aqueous solution and exists in the form of flexible, extended coils. The coil-to-globule transition of PNIPAM is reversible [22, 23]; its driving force is somehow related to the temperature-dependent molecular interactions of PNIPAM, particularly hydrogen bonding and hydrophobic interactions [24]. When PNIPAM is dissolved in an aqueous solvent the water molecules exist in either a free state or bound within the polymer chains [25–27]. The bound water molecules can be also divided into two types: ones that hydrate the hydrophobic groups (e.g., methyl groups or main chain hydrocarbon units) [28–32]; and ones that form hydrogen bonds with C=O or NH groups [23, 28]. The temperature-dependence of PNIPAM has been studied previously using various techniques, including light scattering, differential scanning calorimetry (DSC),

FTIR spectroscopy and turbidimetry; the effect of the solvent composition in mixed aqueous solutions has rarely been investigated [17, 19, 33, 34]. For example, Schild et al. found that the LCST of PNIPAM in pure water is 30–33 °C, but this value changes upon the addition of MeOH, dioxane or THF [17]. They suggested that the LCST of PNIPAM and accompanying changes in polymer conformation result from a balance between hydrogen bonding and hydrophobic effects in aqueous solutions. In this study we used FTIR spectroscopy to examine the hydrogen bonding and hydrophobic interactions of PNIPAM in mixed solvents comprising THF-d_8 and D_2O. Changes in the FTIR spectra revealed information regarding the conformations and bonding states of the functional groups involved in the phase transition; in addition, we could also examine the interactions among the polymer chains and their surrounding THF-d_8/D_2O molecules during the phase transition.

Experimental section

Materials

2-Dodecylsulfanylthiocarbonylsulfanyl-2-methyl propionic acid (DMP) was prepared according the literature procedure [35]. *N*-Isopropylacrylamide (TCI Chemical, Japan) was recrystallized three times from toluene/hexane. 2,2′-azobis(4-methoxy -2,4-dimethylvaleronitrile) (V-70) was purchased from Wako Pure Chemical Industries and used as received. All other solvents and analytical reagents were purchased from commercial suppliers and used as received.

PNIPAM homopolymer [36]

PNIPAM was synthesized in *N*,*N*-dimethylformamide (DMF) employing a conventional azoinitiator, namely 2,2′-azobis(4-methoxy-2,4-dimethylvaleronitrile) (V-70), as the source of primary radicals and DMP, a trithiocarbonate-based CTA. All polymerizations were conducted at 25 °C under a N_2 atm at 33 wt% monomer in a 20-mL dried Schlenk flask. The CTA:monomer ratio ($[CTA]_0/[M]_0$=1:200) was such that the theoretical value of M_n at 100 % conversion was 22,600. The $[CTA]_0/[I]_0$ ratio was 10:1.

Characterization

Molecular weights and molecular weight distributions were determined through gel permeation chromatography (GPC) using a Waters 510 high-performance liquid chromatograph equipped with a 410 differential refractometer, a refractive index (RI) detector and three Ultrastyragel columns (100, 500, and 10^3 Å) connected in series in order of increasing pore size. DMF was the eluent at a flow rate of 1 mL/min. The molecular weight calibration curve was obtained using PEO standards. The GPC traces of the PNIPAM revealed a narrow polydispersity (M_w/M_n) of 1.10 and a value of M_w of 34,250. FTIR spectra were recorded using a Nicolet Avatar 320 FTIR spectrometer equipped with a mercury–cadmium–telluride detector. A solution containing 5 wt % (*w*/*v*) PNIPAM was prepared in a mixed solvent of THF-d_8/D_2O. This solution was equilibrated in a refrigerator for more than 24 h at a temperature below the LCST. An aliquot of the solution was placed into a 5-μm Teflon spacer between two CaF_2 plates that were attached to a metal holder with a circulating water bath at 25 °C. The sample was subjected to these conditions for 10 min prior to data acquisition. For each spectrum, 32 scans were recorded at a resolution of 1 cm^{-1} for both the sample and the background; the accuracy was 1 cm^{-1}. The spectra of each sample were corrected by subtraction of the solvent spectrum recorded under the same conditions. The subtraction was considered satisfactory when the spectrum was flat between 1,750 and 2,650 cm^{-1}. The region between 1,700 and 1,600 cm^{-1} of the corrected spectra was Fourier self-deconvolved to identify the number of components in the amide I band. Subsequently, the amide I band was curve-fitted using Peak Solve software. Finally, the area of each component was transformed into the percentage of each type of C=O group. The optical transmittance of the PNIPAM solutions at a wavelength of 500 nm was measured using an Agilent 8453 UV–Vis spectrophotometer upon increasing the volume fraction of THF-d_8. The concentration of PNIPAM in the solution and the temperature were controlled at 0.3 g/L and 25 °C, respectively. The cloud point was defined as the content of PNIPAM in solution corresponding to a 50 % decrease in transmittance.

Results and discussion

Changes in the C–H stretching bands of PNIPAM in THF-d_8/D_2O

It has been established previously that PNIPAM molecules can undergo a reentrant transition upon increasing the THF content in mixed THF/H_2O solvents. Schild et al. reported that PNIPAM is soluble in both THF and water at room temperature (25 °C), but becomes heterogeneous at a THF volume fraction of approximately 20–65 % [12]. To eliminate complications arising from overlap of the signals of PNIPAM with those for C–H stretching of THF at 2,800–3,000 cm^{-1} and for the O–H band of H_2O near 1,640 cm^{-1}, we employed THF-d_8/D_2O, rather than THF/H_2O, as our mixed solvent for recording FTIR spectra for this present study. Although we suspected that an isotope effect might exist to influence the transition behavior of PNIPAM in the aqueous and deuterated

aqueous solutions, it has been reported that the LCST of PNIPAM in D_2O is only approximately 0.7 °C higher than that in H_2O, with the magnitude of the hysteresis of the transition temperature being unaffected (or only weakly affected) by isotopic substitution [32]. Thus, we suspected that the phase transition behavior and the environment of PNIPAM in THF-d_8/D_2O would be similar to that in THF/H_2O. Figure 1 presents the optical transmittance of the PNIPAM solutions at a wavelength of 500 nm plotted with respect to the volume fraction of THF-d_8. Here, we define the cloud point as the content of the PNIPAM solution corresponding to a 50 % decrease in transmittance. The transmittance of the PNIPAM solutions in D_2O/THF-d_8 at 25 °C revealed that this mixed solvent was a poor solvent when the volume fraction of THF-d_8 (x_v) was in the range from 11 to 55 %; this behavior was almost identical to that for PNIPAM in THF/H_2O mixtures.

Figure 2 presents the selected composition dependence of the absorption bands of the C–H units for 5 wt % PNIPAM in THF-d_8/D_2O. We recorded these spectra for PNIPAM solutions in the ν_{C-H} region as a function of x_v at 25 °C to avoid the effect of temperature on the PNIPAM molecular structure. We assign the absorption bands centered at 2,981 and 2,881 cm^{-1} to the asymmetric [$\nu_{as}(CH_3)$] and symmetric [$\nu_s(CH_3)$] vibrations, respectively, of the methyl groups of the *N*-isopropyl units. The absorption band centered at 2,938 cm^{-1} [$\nu_{as}(CH_2)$] was associated with the asymmetric vibration of the main chains. Thus, a red-shift occurred in the asymmetric vibration of the methyl groups of the *N*-isopropyl units and of the C–H stretching vibration of the main chains. A number of previous

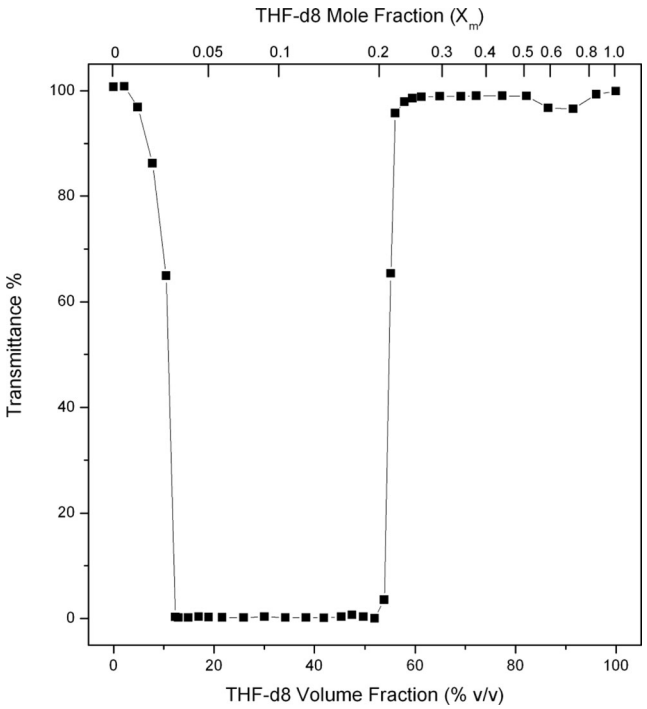

Fig. 1 Optical transmittance at 500 nm plotted with respect to the volume fraction of THF-d_8 for a solution of PNIPAM (3 g/L) in D_2O/THF-d_8

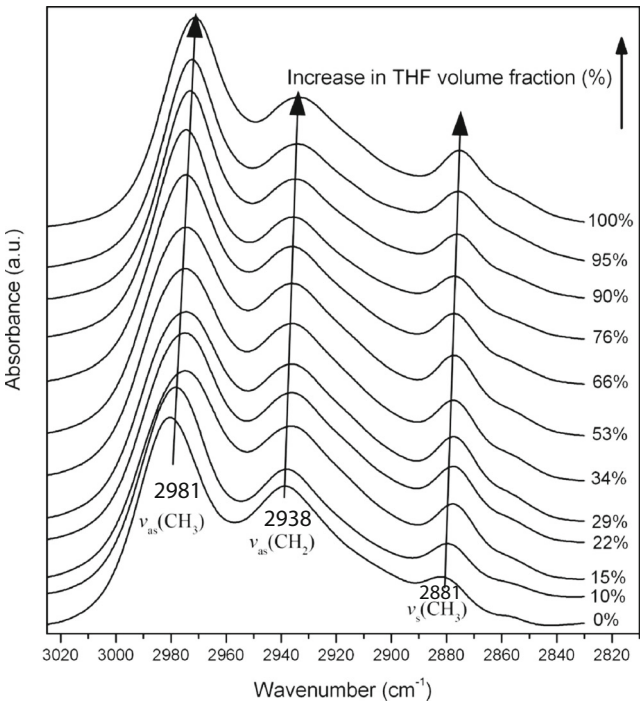

Figure 2 FTIR spectra (ν_{C-H} region) of PNIPAM recorded at 25 °C at various volume fractions of THF-d_8 in mixed solutions of THF-d_8 and D_2O

experiments have revealed that the signal for C–H stretching is blue-shifted with decreased intensity upon interaction with water when the value of x_v increases in solution [27, 28]. Therefore, the red-shift of our IR band indicates that an increase in the THD-d_8 content led to partial dehydration of the CH_3 and CH_2 groups of the PNIPAM chain. Shifts in the values of $\nu_{as}(CH_3)$, $\nu_s(CH_3)$, and $\nu_{as}(CH_2)$ to lower frequencies induced by dehydration of the polymer chain has also been observed previously in the phase transition of the triblock copolymer poly(ethylene oxide)-poly(propylene oxide)-poly(ethylene oxide) [37]. Figure 3 presents a plot of the wavenumbers of the maxima of the signals of $\nu_{as}(CH_3)$, $\nu_s(CH_3)$, and $\nu_{as}(CH_2)$ in PNIPAM solutions with respect to the value of x_v; these signals are useful probes for monitoring the organizational changes of the alkyl chains of PNIPAM. We observed three distinct changes for these signals. First, the signals for $\nu_{as}(CH_3)$, $\nu_s(CH_3)$, and $\nu_{as}(CH_2)$ all shifted toward a lower frequency upon increasing the value of x_v from 0 to 15 %. Next the positions of the signals for $\nu_{as}(CH_3)$ and $\nu_{as}(CH_2)$ remained almost unchanged upon increasing the value of x_v from 15 to 72 %. Finally, the signals for $\nu_{as}(CH_3)$ and $\nu_{as}(CH_2)$ underwent red-shifts when the value of x_v was greater than 72 %.

Changes in the amide I bands of PNIPAM in THF-d_8/D_2O

Because amide groups were present in the PNIPAM structure we attribute the absorption bands centered near 1,670, 1,649,

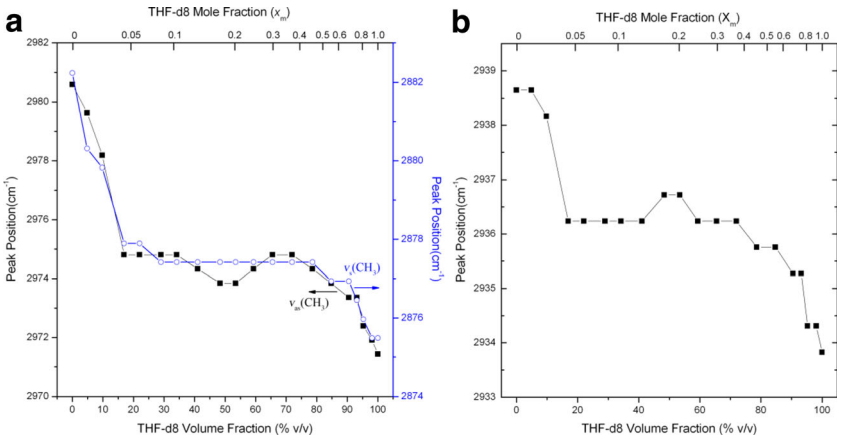

Fig. 3 Peak positions of (**a**) asymmetric (*black square*) and symmetric (*white circle*) C–H stretching vibrations of the methyl groups of PNIPAM, plotted with respect to the volume fraction of THF-d_8; (**b**) Asymmetric C–H (*black square*) stretching vibration of the methylene groups of the backbone of PNIPAM, plotted with respect to the volume fraction of THF-d_8

and 1,625 cm^{-1} to amide I (free C=O), amide I [C=O hydrogen bonded with NH, ν(C=O···H–N)] and amide I [C=O hydrogen bonded with D_2O, ν(C=O···D–OD)] vibrations, respectively [27, 28, 38]. Figure 4 presents selected FTIR spectra of the amide I bands of the PNIPAM chain at various values of x_v. When we increased the value of x_v from 0 to 93 % the intensity of the signal for ν(C=O···D–OD) at 1,624 cm^{-1} decreased while that at 1,649 cm^{-1}, which is attributed to ν(C=O···H–N), increased. When we increased the value of x_v to greater than 95 % the intensity of the free amide I band at 1,670 cm^{-1} rose dramatically while those of the signals for ν(C=O···H–N) and ν(C=O···D–OD) both decreased. Finally, the signal for the C=O units hydrogen bonded to D_2O vanished when the value of x_v reached 100 %.

We curve-fitted the signals for the amide I bands in from 1,700 to 1,600 cm^{-1} to allow a more quantitative analysis. Assuming that the free C=O, C=O···H–N and C=O···D–OD units all contributed to the IR spectra with similar intensities we estimated the area fractions of the free C=O units and the intra- and inter-chain hydrogen bonded C=O units from their ratios of the total peak area [A(1,670)+A(1,649)+A(1,625)]; we obtained two Gaussian peaks through nonlinear fitting of the overlapped amide I region of the spectrum as shown in Table 1. Figure 5 plots the variations of the peak area ratios of three amide I bands of PNIPAM with respect to the value of x_v in the various mixed solvents. For PNIPAM in pure D_2O most of the C=O groups (ca. 77.3 %) were involved in intermolecular hydrogen bonding between the polymer and D_2O molecules. The peak area for intermolecular hydrogen bonding between the polymer and D_2O molecules experienced four states: (i) the peak area of the signal for ν(C=O···D–OD) initially decreased slightly from 77.3 to 75.0 % upon increasing the value of x_v from 0 to 10 %; (ii) the degree of intermolecular hydrogen bonding between the polymer and the solvent molecules suddenly decreased to 61.3 % upon increasing the value of x_v from 10 to 15 %; (iii) the rate of decrease in the area of the signal for ν(C=O···D–OD) decreased to a relatively low, but constant, value upon increasing the value of x_v from 15 to 72 %; (iv) t values of x_v greater than 72 % the rate of decrease of the area of the signal for ν(C=O···D–OD) increased again, ultimately leading to disappearance of this signal.

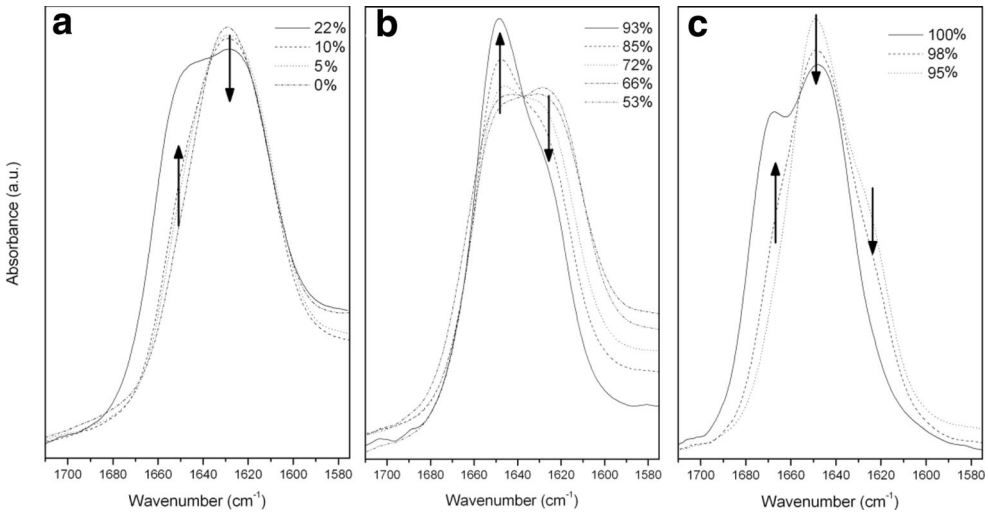

Fig. 4 FTIR spectra (amide I region) of PNIPAM recorded at 25 °C at various volume fractions of THF-d_8 in mixed solutions of THF-d_8 and D_2O. The absorption bands centered near 1,670, 1,649, and 1,625 cm^{-1} are attributed to amide I (free C=O), amide I [C=O hydrogen bonded with N–H, ν(C=O···H–N)] and amide I [C=O hydrogen bonded with D-O-D, ν(C=O···D–OD)] vibrations

Table 1 Peak positions of the hydrated groups in the amide I region of the IR spectra of PNIPAM and curve-fitting data

THF volume fraction (%)	Peak position of $\nu_{as}(CH_3)$ (cm^{-1})	Peak position of $\nu_{as}(CH_2)$ (cm^{-1})	Peak position of $\nu_s(CH_3)$ (cm^{-1})	$A(1,625)^a$ (%)	$A(1,649)^a$ (%)	$A(1,670)^a$ (%)
0	2,980.6	2,938.6	2,882.2	77.3	22.7	–
5	2,979.6	2,938.6	2,880.3	76.5	23.5	–
10	2,978.2	2,938.1	2,879.8	75.0	25.0	–
15	2,974.8	2,936.2	2,877.9	61.3	38.7	–
22	2,974.8	2,936.2	2,877.9	60.3	39.7	–
29	2,974.8	2,936.2	2,877.4	62.4	37.6	–
34	2,974.8	2,936.2	2,877.4	59.7	40.3	–
41	2,974.3	2,936.2	2,877.4	55.8	44.2	–
48	2,973.8	2,936.7	2,877.4	56.4	43.6	–
53	2,973.8	2,936.7	2,877.4	53.2	46.8	–
59	2,974.3	2,936.2	2,877.4	54.3	45.7	–
65	2,974.8	2,936.2	2,877.4	49.5	50.5	–
72	2,974.8	2,936.2	2,877.4	51.9	48.1	–
79	2,974.3	2,935.8	2,877.4	45.4	54.6	–
85	2,973.8	2,935.8	2,876.9	42.6	57.4	–
90	2,973.3	2,935.3	2,876.9	31.0	69.0	0.0
93	2,973.3	2,935.3	2,876.5	35.4	62.7	1.9
95	2,972.4	2,934.3	2,876.0	25.7	71.9	2.4
98	2,971.9	2,934.3	2,875.5	14.0	81.7	4.3
100	2,971.4	2,933.8	2,875.5	0.0	72.3	27.7

[a] $A(1,625)$, $A(1,649)$, and $A(1,670)$ denote the area fractions of the amide I signals of the [C=O···D–OD], [C=O···H–N], and free C=O groups, respectively

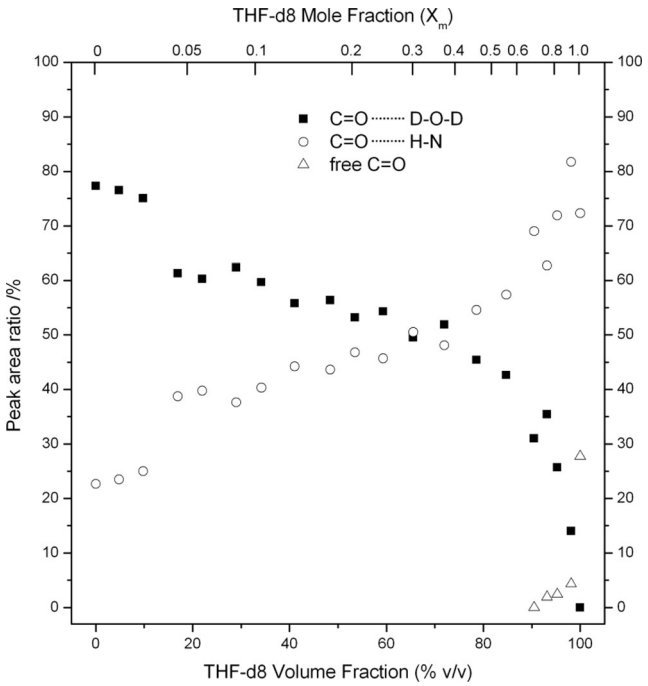

Fig. 5 Peak area ratios of the three components of the amide I band of PNIPAM, plotted with respect to the volume fraction of THF-d_8. (*black square*: Intermolecular hydrogen bonding between PNIPAM and solvent molecules; *white circle*: intra- and interchain hydrogen bonding of PNIPAM; △: free C=O groups of PNIPAM

Change in phase behavior of poly(N-isopropylacrylamide) in THF-d_8/D_2O

To understand the transition behavior of PNIPAM in THF/H_2O we must first distinguish the interactions among THF-d_8, D_2O and the PNIPAM polymer chains. For a solution of PNIPAM in THF-d_8 and D_2O we would expect many kinds of interactions, including hydration of THF-d_8; hydration of the CH_3 and CH_2 groups of PNIPAM chains; hydrophobic–hydrophobic interactions between THF-d_8 and the hydrophobic groups of PNIPAM; hydrogen bonding of C=O and N–H units with D_2O; and hydrogen bonding of C=O units with H–N units. The hydration interaction is about in an order of magnitude stronger than the hydrophobic–hydrophobic interactions (van der Waals, dispersion forces), but is weaker than a hydrogen bond.

As shown in Figs. 2 and 3, the hydrophobic groups of PNIPAM dehydrated readily upon increasing the value of x_v from 0 to 10 %, indicating that the hydration interaction of a THF-d_8 molecule is a stronger than that of the hydrophobic groups of PNIPAM. Because the steric bulk of a PNIPAM chain is higher than that of a single THF-d_8 molecule the effect of steric hindrance lowers the hydration force between the hydrophobic groups of PNIPAM and D_2O. Recent studies on the hydration of THF have revealed that a single THF molecule can complex with several water molecules to form a THF hydration sphere when the THF content is low [39]; in contrast,

at high THF contents, the ratio becomes 1:1. Thus, we conclude that when the value of x_v is less than 10 %, the D_2O molecules form a hydration sphere structure with THF-d_8 prior to hydrating the hydrophobic units of PNIPAM. In addition, the rate of dehydration was greater and the signals for $\nu_{as}(CH_3)$ and $\nu_s(CH_3)$ responded more rapidly than that for $\nu_{as}(CH_2)$, *suggesting that the change in hydration of the CH_3 groups occurred prior to that of the CH_2 groups.*

In addition, we noted that the area of the signal for ν(C=O···H–N) grew slightly at the expense of that for ν(C=O···D–OD) upon increasing the value of x_v from 0 to 10 %. The area of the signal for ν(C=O···D–OD) decreased remarkably upon increasing the value of x_v from 10 to 15 %. This result indicates that an increase in the content of THF-d_8 resulted in a lack of sufficient hydration for the CH_3 and CH_2 groups interacting with D_2O molecules. The main chains of PNIPAM follow by diffusion and aggregation. The hydrophobic groups then aggregated to form hydrophobic cages that prevented the diffusion of D_2O molecules and the formation of hydrogen bonds with the C=O or N–H groups. Scheme 1 presents the probable changes in phase behavior for PNIPAM in THF-d_8/D_2O.

The PNIPAM chains tended to sequence aggregate and form a globular conformation upon increasing the x_v from 11 to 55 %, as displayed in Fig. 1. In this region, the area of the signal for ν(C=O···D–OD) continued to decrease steadily at a relatlyive low but constant value while the positions of the signals for $\nu_{as}(CH_3)$ and $\nu_{as}(CH_2)$ remained almost unchanged. This result indicates that some D_2O molecules were still hydrating the hydrophobic groups of PNIPAM with competition between hydration of the hydrophobic groups of PNIPAM and THF-d_8 molecules creating an equilibrium state. Figure 6 displays the selected ν(C–D) stretching region and the peak position of THF-d_8 in the FTIR spectra as a function of x_v. We found that the THF-d_8 molecules became almost completely dehydrated at a linearly decreasing rate upon increasing the x_v of the PNIPAM solution. This behavior suggests that the hydration sphere structure of THF-d_8 changed from a saturated hydrate form to an unsaturated hydrate and finally to a non-hydrate structure (THF-d_8·$n$$D_2O$) [39]. The hydration sphere of THF-d_8 also hindered the hydrophobic–hydrophobic interactions among THD-d_8 and the hydrophobic groups of PNIPAM; consequently, the PNIPAM strands continued to shrink to form aggregates. The

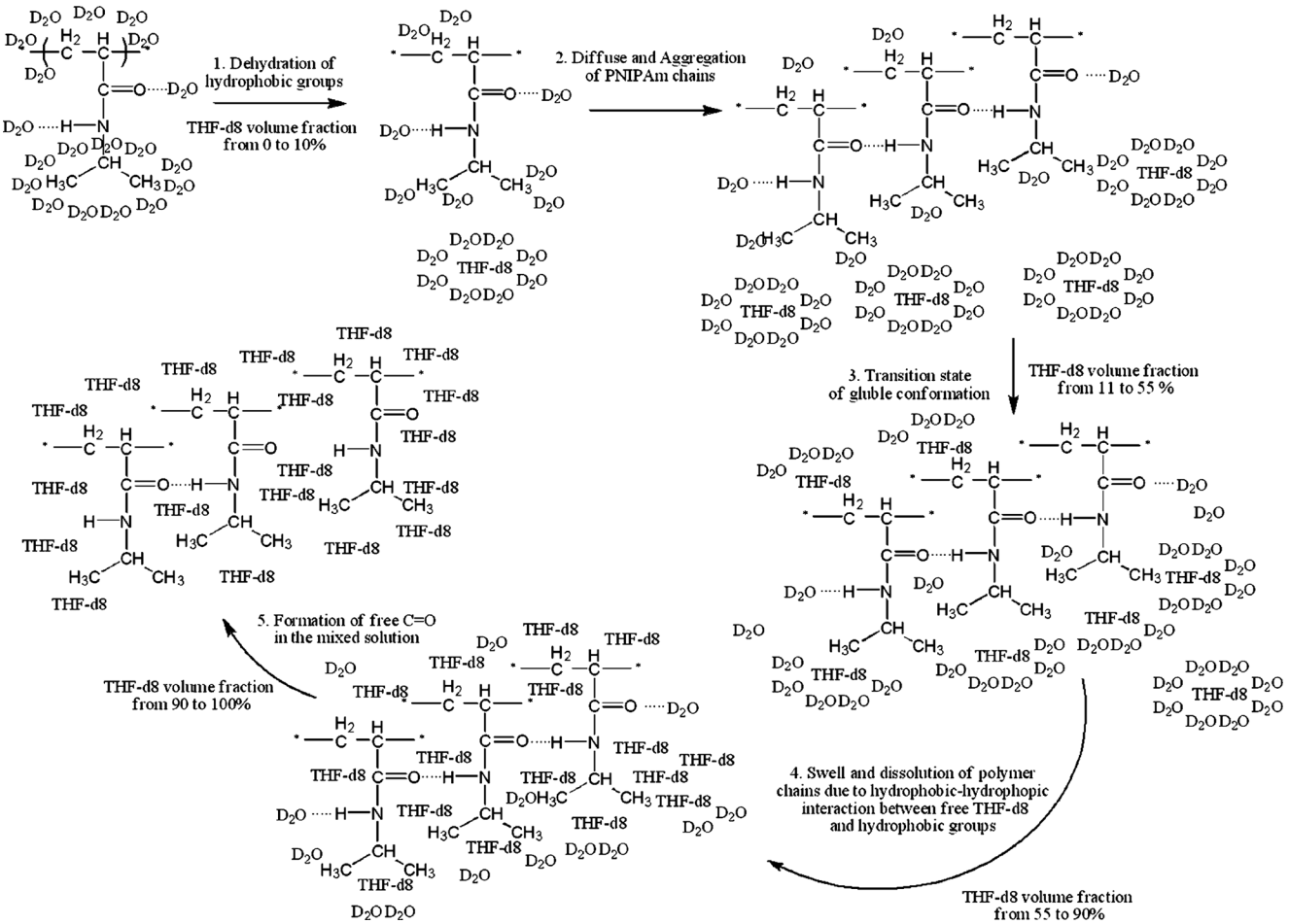

Scheme 1 Schematic representation of the changes in morphology of PNIPAM upon changing the composition of THF-d_8/D_2O

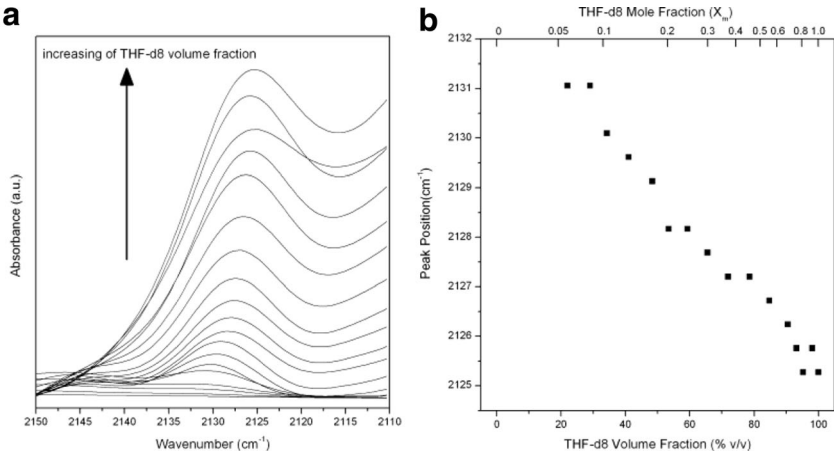

Fig. 6 **a** FTIR spectra (ν_{C-D} region) of PNIPAM solutions recorded at 25 °C at various volume fractions of THF-d_8; **b** Peak position of the signal for ν(C–D) for the PNIPAM solution plotted with respect to the volume fraction of THF-d_8

decrease in signal area for ν(C=O···D–OD) was probably due to the increase in the content of THF hydrate structures even through the hydrogen bonds are stronger than the hydration force.

The PNIPAM chain reentrant formed the coil conformation when the value of x_v was greater than 55 %. In this region almost all of the THF-d_8 molecules having the non-clathrate hydrate structures coexisted within THF-d_8/D_2O complexes and would expose a partial number of the hydrophobic groups in the PNIPAM solution. Because of hydrophobic–hydrophobic interactions among free THF-d_8 molecules and the hydrophobic groups of PNIPAM the CH_3 groups of the *N*-isopropyl units and the CH_2 groups of the main chains of PNIPAM could undergo swelling and then redissolving in the THF-d_8–rich region.

Interestingly, the intensity and area of the signal for ν(C=O···D–OD) also decreased while those of ν(C=O···H-N) increas. A new band that we attribute to free C=O groups appeared at 1,670 cm^{-1} when the value of x_v was greater than 95 %. The peak area fraction of the free C=O groups of PNIPAM in pure THF-d_8 solution was 27.7 %, but it decreased dramatically to 4.3 % upon decreasing the value of x_v to 98 %. This finding indicates that PNIPAM chains can be dissolved in THF-d_8 as a result of hydrophobic–hydrophobic interactions between the solvent and the hydrophobic functional groups without forming hydrogen bonds between C=O groups. The added D_2O molecules readily formed hydrogen bonds with the C=O groups because of the highly extended coils present in the PNIAPM solution resulting in the absence of free amide I groups. Here we also need to emphasize that this behavior may also use desolvation instead of dehydration in the mixed solvent and that the system becomes complicated in this ternary system. In conclusion, it seems that inter- and intrachain hydrogen bonding of the PNIPAM chains do not lead to or affect the morphological changes in the mixed solution even when the signal area for ν(C=O···H–N) was greater than 45 % at values of x_v from 55 to 98 %. In this study we propose that dehydration of the hydrophobic groups rather than inter- and intrachain hydrogen bonding was likely to be the major driving force for the subsequent aggregation and coil-to-globule transition.

Conclusions

We have used FTIR spectroscopy to study the solution behavior of PNIPAM in a mixed solvent of D_2O and THF-d_8. Changes in the spectral data of the CH_3 groups of the *N*-isopropyl amide units and the CH_2 groups of the main chains, as well as the amide I region of PNIPAM, revealed information regarding the hydrophobic and hydrophilic interactions in the mixed aqueous solution. Upon increasing the value of x_v from 0 to 10 % the CH_2 and CH_3 groups of the polymer chains became dehydrated; the PNIPAM chains then gradually aggregated until ultimately collapsing to form a globular conformation. When the value of x_v was in the range from 11 to 55 % the hydrophobic groups aggregated to form hydrophobic cages that prevented the diffusion of D_2O molecules and the formation of hydrogen bonds. Meanwhile, the THF-d_8 hydration sphere also hindered the hydrophobic–hydrophobic interactions among THD-d_8 molecules and the hydrophobic groups of PNIPAM; consequently, PNIPAM continued to shrink to form aggregates. When the value of x_v was greater than 55 % the PNIPAM solution became homogeneous again as a result of hydrophobic–hydrophobic interactions among the free THD-d_8 molecules and the hydrophobic groups of PNIPAM. In contrast, increases in the area fractions for the intra- and interchain hydrogen bonds of PNIPAM did not affect the homogeneity of the PNIPAM solution when the value of x_v was greater than 55 %. We believe that dehydration of the hydrophobic groups rather than inter- and intrachain hydrogen bonding was the major driving force for the subsequent aggregation and coil-to-globule transition.

Acknowledgments This study was supported financially by the National Science Council, Taiwan, Republic of China, under contracts NSC 100-2221-E-110-029-MY3 and NSC 102-2221-E-110-008-MY3. The authors would thank their advisor, Professor Feng-Chih Chang, for his kind help and discussion for this study and for his life. The authors would like to acknowledge the support from the Energy Fund of Ministry of Economics Affairs, Taiwan.

References

1. Biju R, Nair CPR (2013) J Polym Res 20:82
2. Basak D, Ghosh S (2013) ACS Macro Lett 2:799
3. Okano T, Kikuchi A, Sakurai Y, Takei Y, Ogata N (1995) J Control Release 36:125–133
4. Yang HW, Chen JK, Cheng CC, Kuo SW (2013) Appl Surf Sci 271: 60–69
5. Fu HK, Kuo SW, Huang CF, Chang FC, Lin HC (2009) Polymer 50: 1246–1250
6. Zhang Y, Jiang M, Zhao J, Ren X, Chen D, Zhang G (2005) Adv Funct Mater 15:695–699
7. Abdel-Mohdy HL (2013) J Polym Res 20:206
8. Tu CW, Kuo SW, Chang FC (2009) Polymer 50:2958–2966
9. Lai CT, Chien RH, Kuo SW, Hong JL (2011) Macromolecules 44: 6546–6556
10. Chen HW, Li JF, Ding YW, Zhang GZ, Zhang QJ, Wu C (2005) Macromolecules 38:4403–4408
11. Asrnarandei I, Fundueanu G, Cristea M, Harabagiu V, Constantin M (2013) J Polym Res 20:293
12. Percot A, Lafleur M, Zhu XX (2000) Polymer 41:7231–7239
13. Dhara D, Chatterji PR (2000) Polymer 41:6133–6143
14. Sagle LB, Zhang Y, Litosh VA, Chen X, Cho Y, Cremer PS (2009) J Am Chem Soc 131:9304–9310
15. Lin SY, Chen KS, Liang RC (1999) Polymer 40:2619–2624
16. Percot A, Zhu XX, Lafleur M (2000) J Polym Sci Part B: Polym Phys 38:907–915
17. Schild HG, Muthukumar M, Tirrell DA (1991) Macromolecules 24: 948–952
18. Mukae K, Sakurai S, Sawamura S, Makino K, Kim SW, Udea I, Shirahama K (1993) J Phys Chem 97:737–741
19. Winnik FM, Ottaviani MF, Bossmann SH, Garciagaribay M, Turro NJ (1992) Macromolecules 25:6007–6017
20. Amiya T, Hirkawa Y, Hirose Y, Li Y, Tanak T (1987) J Chem Phys 86:2375
21. Zhang G, Wu C (2001) J Am Chem Soc 123:1376–1380
22. Maeda Y, Nakamura T, Ikeda I (2001) Macromolecules 34:8246–8251
23. Cheng H, Shen L, Wu C (2006) Macromolecules 39:2325–2329
24. Siu M, Liu HY, Zhu XX, Wu C (2003) Macromolecules 36:2103–2107
25. Corkhill PH, Jolly AM, Ng CO, Tighe BJ (1987) Polymer 28:1758–1766
26. Barnes A, Corkhill PH, Tighe BJ (1988) Polymer 29:2191–2202
27. Sun B, Lin Y, Wu P, Siesler HW (2008) Macromolecules 41:1512–1520
28. Maeda Y, Higuchi T, Ikeda I (2000) Langmuir 16:7503–7509
29. Stillinger FH (1980) Science 209:451–457
30. Israelachvili J, Pashley R (1982) Nature 300:341–342
31. Inomata H, Goto S, Saito S (1990) Macromolecules 23:4887–4888
32. Cho EC, Lee J, Cho K (2003) Macromolecules 36:9929–9934
33. Liu MZ, Bian FL, Sheng FL (2005) Eur Polym J 41:283–291
34. Winnik FM, Ringsdorf H, Venzmer J (1990) Macromolecules 23: 2415–2416
35. Lai JT, Filla D, Shea R (2002) Macromolecules 35:6754–6756
36. Convertine AJ, Ayres N, Scales CW, Lowe AB, McCormick CL (2004) Biomacromolecules 5:1177–1180
37. Guo C, Wang J, Liu H, Chen JY (1999) Langmuir 15:2703–2708
38. Maeda Y, Higuchi T, Ikeda I (2001) Langmuir 17:7535–7539
39. Manakov AY, Goryainov SV, Likhacheva AY, Fursenko BA, Dyadin YA, Kurnosov V (2000) Mendeleev Commun 10:80–81